Design of Oxide Inclusion and Fluidity Measuring Instruments in Aluminum Alloy

Donanta Dhaneswara
Department of Metallurgical and Materials Engineering, Universitas Indonesia

Azzahra Febrianti Mulyo
Department of Metallurgical and Materials Engineering, Universitas Indonesia

Ahmad Azhari
Department of Metallurgical and Materials Engineering, Universitas Indonesia

Muhammad Anis
Department of Metallurgical and Materials Engineering, Universitas Indonesia

他

https://doi.org/10.5109/7326966

出版情報：Evergreen. 11 (4), pp.3316-3324, 2024-12. 九州大学グリーンテクノロジー研究教育センター
バージョン：

Design of Oxide Inclusion and Fluidity Measuring Instruments in Aluminum Alloy

Donanta Dhaneswara[1,*], Azzahra Febrianti Mulyo[1,*], Ahmad Azhari[1], Muhammad Anis[1], Bambang Suharno[1], Andrew Suharli[1], Kristanto Wahyudi[2]

[1]Department of Metallurgical and Materials Engineering, Universitas Indonesia, Kampus UI Depok, Jawa Barat, 16424, Indonesia.

[2]Balai Besar Standardisasi dan Pelayanan Jasa Industri (BPPSPJI) Keramik dan Mineral Non-Logam, Bandung, 40272, Indonesia

*Author to whom correspondence should be addressed:

E-mail: donanta.dhaneswara@ui.ac.id (D. Dhaneswara), azzahrafebriantimulyo@gmail.com (A.F. Mulyo)

(Received October 21, 2023; Revised July 23, 2024; Accepted November 25, 2024).

Abstract: Aluminum has widely been used in automotive industries because of its ability to be recycled. It is concerned that the properties of secondary aluminum are not as good as the primary aluminum because there are many impurities and also low fluidity values that can reduce the quality of aluminum products. To determine inclusions and fluidity values, PodFA and Prefil instruments are currently used, but these instruments are still very expensive in the industry. Therefore, in this research, a progressive oxide inclusion and fluidity value measuring instrument will be designed. To verify the instrument can work according to its standards, this research uses an AC8A aluminum alloy to determine the presence of oxide inclusions and fluidity values. The independent variables used are cast temperature variations of 720˚C, 740˚C, and 760˚C. Based on the results of testing and characterization, it is found that this instrument can accurately and precisely measure the fluidity of aluminum alloy, where the sample with the temperature of 760˚C provides optimum results, with the mass filtered every 10 seconds is 225.94 grams, 500.45 grams, and 682.36 grams. Impurities found in aluminum alloys are Al_2O_3, Al_3Ti, MgO, Al_4C_3, and Si (Refractory Brick).

Keywords: IFMI Instruments; AC8A Aluminum Alloy; Oxide Inclusion; Fluidity

1. Introduction

Aluminum needs has been steadily increasing along with time because of its outstanding properties, such as being lightweight, good electrical and thermal conductivity, and also good corrosion resistance[1)]. In the global market, especially in the automotive industry, the demand for aluminum is high since the industry need lightweight vehicles to improve energy efficiency[2,3)]. Furthermore, secondary aluminum is used to replace the primary aluminum because of their availability is very limited. This is also because the energy consumption required for recycling scrap aluminum is only 5% of primary aluminum. It is expected that the recycling process of scrap aluminum can save up to 95% of energy and contribute to preserving the country's foreign exchange expenditure as domestic production capacity increases[4,5)].

Secondary aluminum (scrap) refers to used aluminum materials that are recycled through melting as raw material for aluminum production[6,7)]. The content of scrap aluminum is no longer as pure as primary aluminum due to the presence of impurities. This often results in oxide inclusions such as MgO, Al_2O_3, Spinel, SiO_2, FeO, and Fe_2O_3 in the scrap[8–10)]. These oxide inclusions remain in the aluminum ingots and can lead to a decrease in surface quality, machineability, and mechanical properties if proper treatment is not carried out[11)]. All of these inclusions can arise due to various reasons, some of which are because of poor refining treatments of molten aluminum, the usage of scrap aluminum that contained impurities, and also improper experimental procedures. Chemical reactions in furnace resulting in more impurities can happen, since the higher the temperature was, the time for phases and elements that are in the aluminum alloy can react with oxygen will be longer[12)]. However, some mitigation could be done to reduce inclusions in aluminum, such as using ceramic foam filter, doing proper refining process such as using flux while melting the metal in furnaces[13,14)].

Consequently, the resulting products from aluminum scrap may not be optimal and not meet the Indonesian National Standards (SNI). Inclusions in liquid metals is one of the factors that can affect fluidity because inclusions are insoluble particles that will significantly reduce the fluidity of liquid metals[15)]. It happens because

the impurities will be a foreign object that will hinder the flow of liquid metals, therefore the flow will not be smooth and it will change the fluidity of molten aluminum.

Fluidity refers to the ability of liquid metals to flow through molds and fill empty spaces in the mold at the metal melting temperature before solidification[16]. Fluidity is an important factor in casting to avoid defects in liquid metals. In the case of aluminum alloy, fluidity is influenced by temperature, composition, inclusions, viscosity, material cleanliness, and rapid cooling processes[16]. However, to improve the fluidity value of aluminum alloys, it is not only influenced by temperature but also by mold diameter and vacuum size[16]. Currently, fluidity testing is carried out using various methods that have been developed, such as the spiral method, vacuum method, and casting industry methods such as PoDFA and Prefil.

To determine the type of inclusions and fluidity value in molten aluminum alloys, instruments such as the Porous Disc Filtration Apparatus (PoDFA) and Pressure Filtration (Prefil) are used. These two instruments serve different functions, where PoDFA provides information about the composition and concentration of inclusions in the liquid metal[17,18], while Prefil determines the fluidity value of the liquid metal[19,20]. However, the PoDFA and Prefil instruments required to determine the type of inclusions and fluidity value are still relatively expensive. Therefore, this research aims to develop an Inclusion and Fluidity Measurement Instrument (IFMI) that can evaluate the cleanliness of liquid metals, provide information about fluidity and the concentration of oxide inclusions present in the metal, and reduce the cost efficiency of purchasing both instruments. This research is conducted using various pouring temperatures in the melting of AC8A alloy, namely 720°C, 740°C, and 760°C, to test the influence of pouring temperature on fluidity and the distribution of oxide inclusions.

2. Materials and Methods

2.1 Materials

During this research, the raw material used was AC8A aluminum alloy that were obtained from an aluminum smelting company, the other material used was scrap aluminum that was obtained from past casting processes in the laboratory. The equipment used in the casting process were crucible, ladles, zircon, furnace and the Inclusion and Fluidity Measuring Instrument (IFMI). The main components for the IFMI assembly were load cells, vacuum pumps, gas hoses, manometers, thermometers, and pressure gauges sourced domestically.

2.2 Experimental

The primary raw material used in this research is AC8A aluminum alloy, which was cut into 5 different parts using band saw. The initial step in this process involved weighing the ingredients using a scale with a composition of 70% or 3.5 kg AC8A aluminum ingots and 30% or 1.5 kg scrap aluminum. Subsequently, the furnace that will be used need to be cleaned first to prevent impurities and ensure the cleanliness of the furnace. The furnace will also be coated with zircon, to minimalize thermal shock and also to prevent molten metal stuck to furnace wall.

The casting process of AC8A aluminum allow involved putting 5 kg of scrap and ingots into the furnace, followed by pre-heating at 200ºC to prevent big thermal shock and thermal gradient. The heating continued until 720ºC, 740ºC, and 760ºC. During the melting process, each temperature increase required a holding time of 30 minutes to made sure that the molten metal has fully liquified. After the aluminum has melted completely, fluxing is needed to completely removed the slag which was in the molten surface. Once the desired temperature is reached, the molten metal is poured into a preheated crucible[21].

The crucible was then placed in the IFMI apparatus for further testing. Before the crucible was placed, IFMI needed to be calibrated to made sure that the settings were compatible. Crucibles are used as containers to contain molten metal. Crucible was also preheated to prevent thermal expansion. Micro filter that was preheated will also be mounted on the base of the crucible. Subsequently, the molten metal is transferred to the crucible at predetermined temperature, and at a stable vacuum of –25 inHg so that the molten metal is forced through the micro filter. Then, the monitor on IFMI will showed a graph illustrating the relationship between fluidity and temperature.

The step marked the final stage of aluminum casting process, resulting in filtered aluminum alloy, this result will be followed by characterization for further examination. SEM (Field emission-SEM FEI Inspect F50) and EDS (Energy Dispersive Spectroscopy) will be done to determine the oxide inclusion formed in the sample, also to see the surface characteristics[22,23]. Optical Microscope (OM) is also used to analyzed detailed sample structures and morphologies[24]. OM is also used to determine the suitable location that contained the desired microstructure for SEM. Lastly, Optical Emission Spectroscopy (OES) was done to identify the element that's in the aluminum alloy, whether it was according to standard or not[25–27].

3. Result and Discussion

3.1 Design and Fabrication of Inclusion and Fluidity Measurement Instrument (IFMI)

The design and fabrication of the inclusion and fluidity measurement instrument (IFMI) are carried out as a substitute product for existing imported products in the aluminum metal casting industry and to minimize the limitations of fluidity testing obtained with spiral, square spiral, and other methods, as can be seen in Figure 1 and Figure 2. The results of the IFMI instrument design are

expected to evaluate the cleanliness of the liquid metal and provide information regarding the fluidity value and the presence of oxide inclusion concentrations in the sample using a pure vacuum method assisted by a ceramic foam filter[28,29].

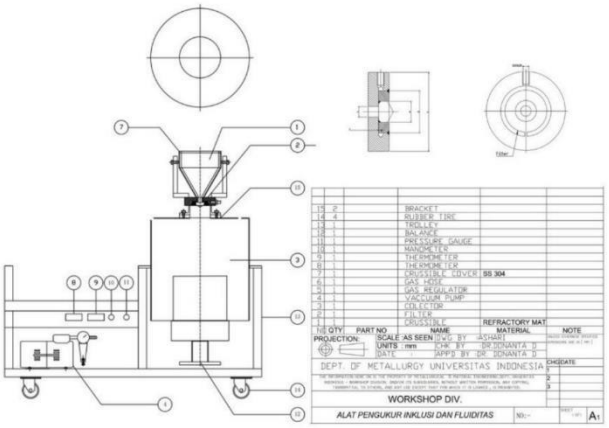

Fig. 1: Description of Component Positions in The Design of IFMI.

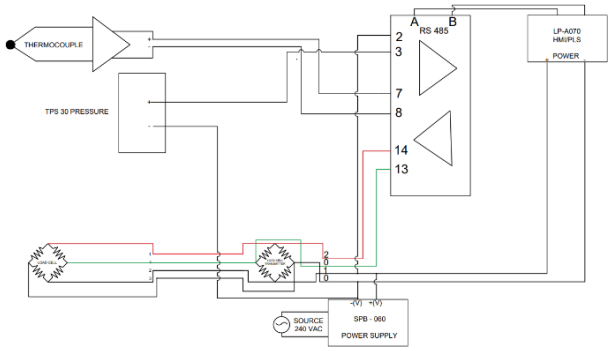

Fig. 2: Single Line Diagram.

The working principle of this inclusion and fluidity measurement instrument consists of two main parts: the vacuum pump control system and the flow monitoring system. The principle of the vacuum pump control system is to maintain the vacuum pressure stored in the vacuum pressure tube (Vacuum Chamber) which is then circulated by a gas hose attached to the rear part of the chamber to suction the liquid aluminum in the crucible positioned above the chamber. On the other hand, the flow monitoring system is used to determine and read the results of the liquid aluminum that is suctioned by the vacuum. The filtered aluminum results will be displayed on the monitor. Additionally, the flow system mentioned in the instrument is also used to regulate the electrical circuitry and sensors within the instrument. The working system and visual appearance of the IFMI instrument can be seen in Figure 3 and Figure 4, respectively.

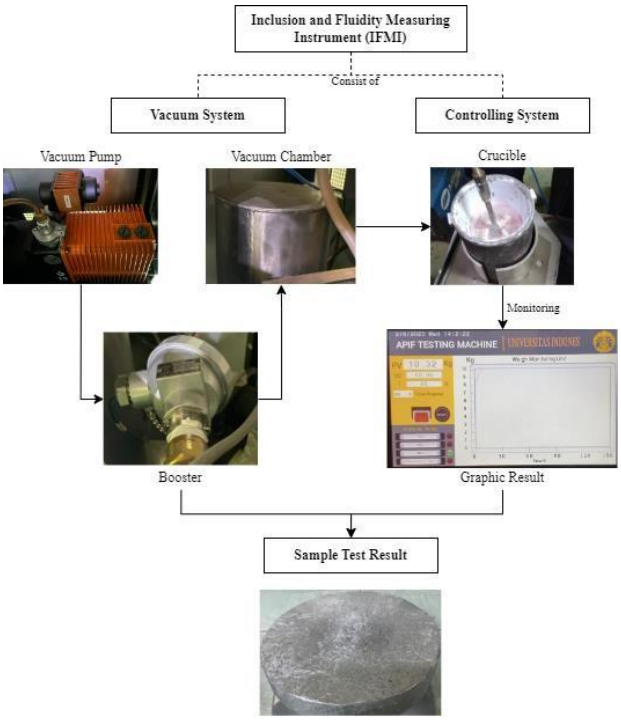

Fig. 3: The Working System of The IFMI Instrument.

Fig. 4: IFMI Instrument.

The design and fabrication of the inclusion and fluidity measurement instrument have fulfilled the expected aspects, including ergonomic aspect, meaning that the instrument is made cheaper and more reliable for testing while maintaining quality. It has consistently proven its ability to filter and measure oxide inclusions and fluidity. The instrument is portable, and also easy to operate. The desired vacuum pressure has been obtained through calibration. IFMI instrument can also be used for various tests such as gas porosity and its effects on fluidity.

3.2 Verification of Inclusion and Fluidity Measurement Instrument (IFMI) by Varying Temperature

Temperature is one of the factors that influence the fluidity value of a metal. The fluidity of liquid metal can affect the microstructure to become finer and prevent defects from occurring. The selection of temperature variations in the verification process is used to consider

the ease factor. The verification testing is conducted by varying the temperature to 720˚C, 740˚C, and 760˚C at a constant vacuum of -25.9 inHg (calibrated result). The material used is AC8A alloy aluminum, which belongs to the aluminum-silicon-magnesium alloy type. The initial process involves preparing the equipment and materials, preparing the casting process, and preparing the IFMI instrument for testing. Subsequently, the fluidity test data is obtained from the data logger of the IFMI instrument and will be processed in the form of a graph showing the relationship between mass and time, as shown in Figure 5. To support the fluidity test data, sample analysis is performed using metallographic testing to observe the microstructure. From the graph in Figure 5, it can be seen that as the temperature of AC8A alloy aluminum increases from 720˚C to 760˚C, the fluidity value also increases.

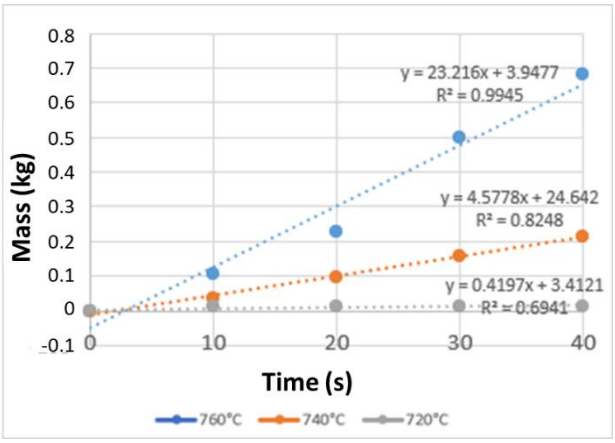

Fig. 5: Fluidity Value Results.

Quantitative analysis of the increase in fluidity value with temperature variation with mass yields the following results: At 720˚C, the mass values obtained are 11.700 grams at 10 seconds, 12.141 grams at 20 seconds, 12.977 grams at 30 seconds, and 13.710 grams at 40 seconds. At 740˚C, the mass values are 33.850 grams at 10 seconds, 97.491 grams at 20 seconds, 135.985 grams at 30 seconds, and 139.760 grams at 40 seconds. At 760˚C, the mass values are 104.400 grams at 10 seconds, 225.940 grams at 20 seconds, 500.450 grams at 30 seconds, and 682.366 grams at 40 seconds. This is in accordance with Zayad M. and Yunus Emre, where the higher the temperature, the fluidity also increases[30,31].

In this case, the results of the fluidity testing show that as the superheat degree increases, the amount of heat that needs to be released before solidification increases. The relationship between mass and time with temperature variation shows that as the temperature increases, the liquid metal is more easily filtered because there is a greater amount of heat that needs to be released, resulting in a larger mass of the liquid metal being filtered with the assistance of the vacuum provided by the IFMI instrument. Therefore, temperature, as one aspect to increase the fluidity value and also decrease the viscosity of the liquid metal, because based on the literature[32] (fluidity is inversely proportional to viscosity). After the testing, the AC8A sample is further cut for microstructure observation using metallographic testing. The microstructure images of the AC8A sample can be seen in Figure 6.

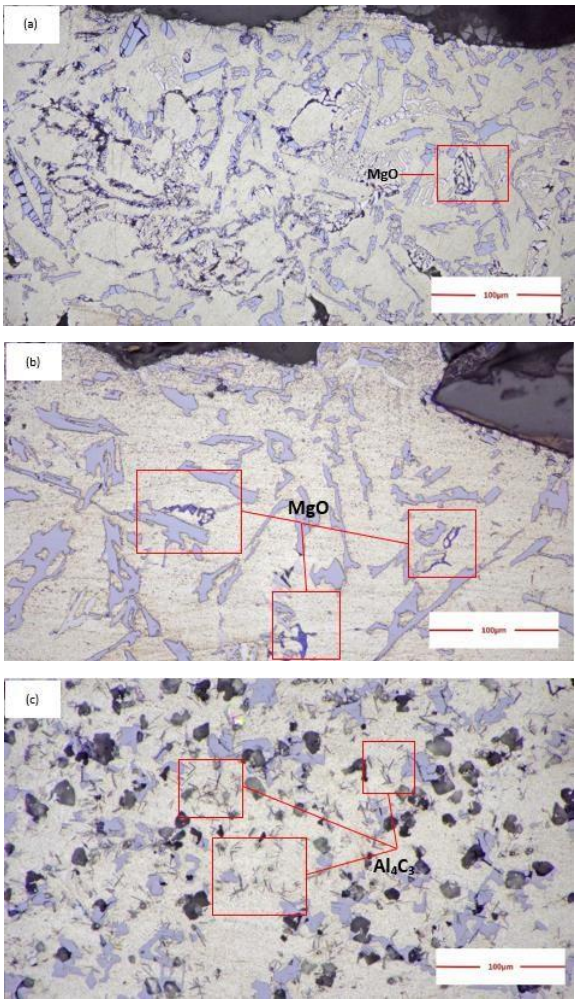

Fig. 6: Microstructure of AC8A Aluminum Alloy at 500x at (a) 720˚C (b) 740˚C (c) 760˚C.

Microstructure testing was conducted using Optical Microscopy (OM) to observe the grain structure formed from the used temperature variations. The OM test began with sample preparation, which involved sequential grinding using sandpaper with grit sizes of 180, 240, 300, 500, 600, 800, 1000, and 1500. Subsequently, polishing was performed using velvet cloth and alumina, followed by etching using Keller's reagent. Figure 6 presents the results of the testing using temperatures of 720˚C, 740˚C, and 760˚C, which showed significant structural changes. Upon examination of the grain size and distribution, it was observed that at 760˚C, the grain size was smaller compared to 720˚C and 740˚C. According to the literature, temperature influences grain size, whereby higher temperatures used during casting result in finer and smaller grains. This, in turn, affects the mechanical properties of aluminum, improving its elongation and making the material more ductile. The microstructure

shows that when the temperature is below 720˚C, the alloy mainly consists of deformed grains, and the degree of recrystallization is minimal. When the temperature rises to 740˚C, the alloy shows a more even distribution of recrystallized grains. However, when the deformation temperature reaches 760˚C, the recrystallized grains tend to become coarse. Therefore, it can be concluded that the degree of recrystallization is strongly influenced by the deformation temperature[33,34].

3.3 Analysis of OES Testing Results

Optical Emissions Spectroscopy (OES) testing needs to be conducted to determine the elemental composition of the metal. OES testing provides data on the actual percentage of elements present in the tested material. Table 1 shows the chemical composition of AC8A aluminum alloy obtained from OES testing. Both chemical compositions align with the range of each element found in AC8A aluminum alloy according to the literature

Table 1. OES Results on AC8A Aluminum Alloy

Elements	Reference	Percentage
Al	≥80%	83.2%
Si	11-13%	12.6%
Fe	≤0.8%	0.194%
Cu	0.8-1.3%	1.17 %
Mn	≤0.15%	0.0346%
Mg	0.7-1.3%	1.29%
Ni	0.8-1.5%	1.30%
Zn	≤0.15%	0.0256%
Pb	≤0.05%	< 0.002%
Ti	≤0.2%	0.0355%

Therefore, the material used in this research conforms to the JIS H5202 and ISO 3522 standards for AC8A aluminum alloy. This confirms the suitability of using AC8A aluminum alloy for casting purposes. The OES testing results indicate that the chemical composition of AC8A aluminum alloy consists of Al-12Si-1Mg, with Al accounting for 83.2%, Si for 12.6%, and Mg for 1.29%.

3.4 Surface Area and Pore Characteristics

Figure 7, shows the results of testing using Scanning Electron Microscopy (SEM) on the three samples obtained from casting AC8A aluminum alloy at different pouring temperatures of 720˚C, 740˚C, and 760˚C. The solid samples are then cut at the bottom for a length of 25mm, followed by metallographic preparation, including mounting, grinding, and polishing, to make the inclusions visible under the microscope[35,36]. In the SEM testing, the surface of the samples was magnified by 5000x. The observed results in Figure 7 align with the findings of previous studies, which identified the presence of various inclusions, such as Al_2O_3, MgO, Spinel, and others, located before the sample filter[37].

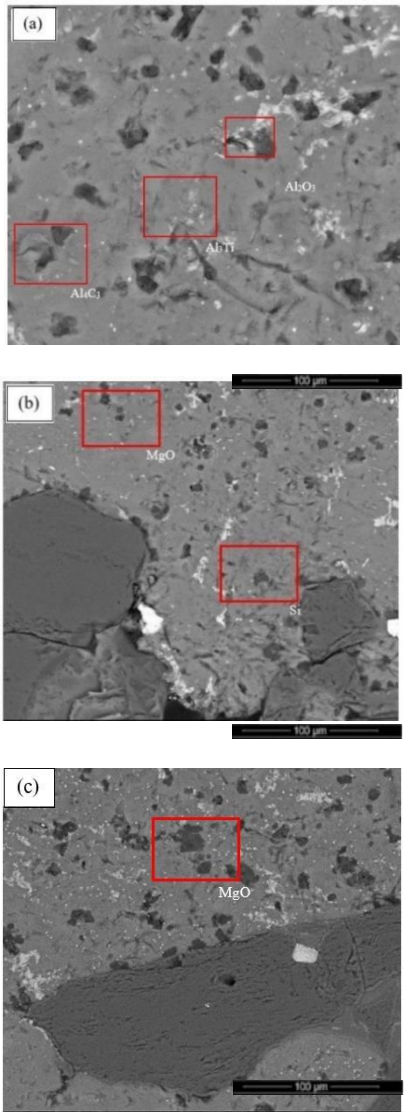

Fig. 7: Analysis of inclusion distribution with SEM-EDS at different pouring temperatures (a) 760˚C, (b) 740˚C, (c) 720˚C for AC8A aluminum alloy casting.

The samples exhibit a significant distribution of inclusions, with a higher concentration of inclusions observed in the AC8A aluminum alloy at a pouring temperature of 760˚C[38,39]. Based on the results in Table 2 of the EDS characterization, the dominant elements in the SEM-EDS analysis were Al at 65.95%, C at 5.24%, and O at 21.79%. According to literature[40,41], these elements can form inclusions such as Al_2O_3, Al_3Ti, and Al_4C_3. Similarly, the EDS characterization in Table 2 confirms the dominance of Al at 65.95%, C at 5.24%, and O at 21.79% in the SEM-EDS analysis.

SEM analysis of the sample with a pouring temperature of 740˚C reveals a uniform distribution of inclusions, primarily consisting of a single type of inclusion. Based on the results in Table 2 of the EDS characterization, the dominant elements in the SEM-EDS analysis were Al at 57.13%, Si at 10.39%, and O at 26.74%. However, there

is also a presence of Mg at 2.05%, indicating the formation of MgO inclusion and Si as refractory brick, as seen in Figure 7, as suggested by literature[40,41].

SEM analysis of the sample with a pouring temperature of 720˚C also shows a uniform distribution of inclusions, predominantly consisting of a single type of inclusion. Based on the results in Table 2 of the EDS characterization, the dominant elements in the SEM-EDS analysis were Al at 51.47%, Si at 9.28%, and O at 31.85%. Additionally, there is the presence of P at 6.09%, indicating the formation of complex compounds with other elements that can be trapped within the crystal structure and cause inclusions. According to literature, these elements can form Al_2O_3 inclusions, as seen in Figure 7.

Table 2. Detected Elements from Point Testing using EDS Analysis Indicating the Formation of Inclusions in AC8A Aluminum Alloy.

Temperature	Inclusion	Element	Weight %	Atomic%
760°C	Al_2O_3 and Al_4C_3	C	5.24	9.76
		O	21.79	30.51
		Al	65.95	54.75
		Si	3.44	2.75
		P	2.35	1.70
		Ca	0.16	0.09
		Ti	0.22	0.10
		Fe	0.84	0.34
	Al_3Ti	C	31.39	53.98
		O	5.13	6.63
		Al	32.66	25.00
		Si	2.79	2.05
		Ca	9.76	5.03
		Ti	8.97	3.87
		Fe	9.30	3.44
740°C	MgO and Si (Refractory Brick)	O	26.74	38.31
		Mg	2.05	1.93
		Al	57.13	48.54
		Si	10.39	8.48
		P	3.69	2.73
720°C	MgO	O	31.85	44.44
		Mg	1.31	1.20
		Al	51.47	42.59
		Si	9.28	7.38
		P	6.09	4.39

3.5 Analysis of The Success of The Inclusion and Fluidity Measurement Device (IFMI)

The success of a testing device is evaluated based on precision and accuracy. Precision refers to the device's ability to produce consistent values in a series of measurement activities, while accuracy is the device's ability to produce values that are close to the true value of the measured quantity. This is due to the random error inherent in any measurement process; factors that affect the measurement results cannot be fully controlled. In practically interpreting measurement data, this variability must be considered. The difference between the test results and some specific values may be within the range of unavoidable random errors, so significant deviations from the set values cannot yet be identified. Calibration is required for measurement devices to compare the measured quantity indicated by the measuring instrument with a more precise standard instrument through an unbroken chain of comparison to the International System of Units (SI). Table 3 and Table 4 presents the results of accuracy and precision testing using standard blocks, respectively.

Table 3. Results of Standard Block Testing to Calculate the Accuracy of the IFMI Device.

Accuracy					
No	Block Reading (kg)			Error Point	Average
1	1	2	3		
2	0.98	0.99	1	1	0.99
3	0.98	0.98	1	2	0.986666667
4	0.98	0.98	1	2	0.986666667
5	0.98	0.98	1	2	0.986666667
6	0.98	0.98	1	2	0.986666667
7	0.98	0.98	1	2	0.986666667
8	0.98	0.98	1	2	0.986666667
9	0.98	0.98	1	2	0.986666667
10	0.98	0.98	1	2	0.986666667
11	0.98	0.98	1	2	0.986666667
12	0.99	1	1	1	0.996666667
	Average				0.987878788
	Standard Deviation				0.003081388
	Blok Standard				1 kg
	Upper Limit				1
	Lower Limit				0.98
	Average error			1.818182	1.82%
	Accuracy				98.181818181818200%

Table 4. Results of Standard Block Testing to Calculate the Precision of the IFMI Device.

Precision	
Measurement Data	
No	Mass Block Reading (1 kg)
1	0.98
2	0.98
3	0.98
4	0.99
5	0.99
6	0.99
7	0.99
8	0.98
9	0.98
10	0.98
11	0.98
12	0.99
Standard Deviation	0.005149287
Average	0.984166667

The results of precision and accuracy testing of the load cell using a standard 1 kg block were conducted to assess the success of the Inclusion and Fluidity Measurement Device as a testing instrument. The calculation results indicate that this device has an accuracy and precision level of 98%, where the standard for accuracy and precision of testing devices is considered accurate when it is above 95%.

4. Conclusion

In conclusion, an oxide inclusion and fluidity measuring instrument (IFMI) designed that able to evaluate the cleanliness of liquid metal and can provide information related to fluidity and the concentration of oxide inclusions contained and also reduce the cost efficiency of existing instruments in the industry is successfully created. The working principle of this fluidity instrument consists of two main parts, the vacuum pump control system and the flow monitor system so that it can work according to its function. Fluidity at 760˚C is higher than the temperature of 720˚C and 740˚C, this is because fluidity is influenced by the pouring temperature where the higher the pouring temperature, the amount of heat that must be released and more, so the higher the fluidity value in AC8A aluminum alloy. The presence of

inclusions in the test material is also influenced by differences in temperature, where the higher the pouring temperature, the fewer inclusions are found in the microstructure. The oxide inclusions that were found in this study is also in accordance to previous research, generally Al_2O_3, Al_3Ti, Al_4C_3, and MgO. The success of the IFMI instrument has been proven by its function to determine the presence of inclusions and measure the fluidity value of liquid aluminum and has been tested from the accuracy and precision measurement results level of 98%.

Acknowledgements

The work was supported by a research grant from Hibah Kedaireka, PKS number: 278/PKS/WRIII-DISTP/UI/2022. The authors would also like to thank Balai Besar Standardisasi dan Pelayanan Jasa Industri (BBSPJI) Keramik dan Mineral Non-logam, Ministry of Industry, Bandung.

References

1) A.K. C, M. Reddy, and M.K. M, "Air jet erosion studies on aluminum-red mud composites using taguchi design," *EVERGREEN*, **10**(1), 130–138 (2023). https://doi.org/10.5109/6781059
2) M.P. Moodispaw, B. Chen, A.A. Luo, and Q. Wang, "Achieving metallurgical bonding in aluminum/steel bimetallic castings," *Int. J. Met.*, **18**(4), 2832-2840 (2024). https://doi.org/10.1007/s40962-023-01241-0.
3) D. Raabe, D. Ponge, P.J. Uggowitzer, M. Roscher, M. Paolantonio, C. Liu, H. Antrekowitsch, E. Kozeschnik, D. Seidmann, B. Gault, F. De Geuser, A. Deschamps, C. Hutchinson, C. Liu, Z. Li, P. Prangnell, J. Robson, P. Shanthraj, S. Vakili, C. Sinclair, L. Bourgeois, and S. Pogatscher, "Making sustainable aluminum by recycling scrap: the science of 'dirty' alloys," *Prog. Mater. Sci.*, **128**, 100947 (2022). https://doi.org/10.1016/j.pmatsci.2022.100947.
4) S. Van den Eynde, E. Bracquené, D. Diaz-Romero, I. Zaplana, B. Engelen, J.R. Duflou, and J.R. Peeters, "Forecasting global aluminium flows to demonstrate the need for improved sorting and recycling methods," *Waste Manag.*, **137**, 231-240 (2022). https://doi.org/10.1016/j.wasman.2021.11.019.
5) D. Baffari, A.P. Reynolds, A. Masnata, L. Fratini, and G. Ingarao, "Friction stir extrusion to recycle aluminum alloys scraps: energy efficiency characterization," *J. Manuf. Process*, **43**, 63-69 (2019). https://doi.org/10.1016/j.jmapro.2019.03.049.
6) R. Yadav, S. Prakash Dwivedi, and V.K. Dwivedi, "Effect of casting parameters on tensile strength of chrome containing leather waste reinforced aluminium based composite using rsm," *EVERGREEN*, **9**(4), 1031–1038 (2022). https://doi.org/10.5109/6625716
7) P. Kumar, V. Sharma, D. Kumar, and S. Akhai, "Morphology and mechanical behavior of friction stirred aluminum surface composite reinforced with graphene," *EVERGREEN*, **10**(1), 105–110 (2023). https://doi.org/10.5109/6781056
8) Y. Fugane, S. Kashiwakura, and K. Wagatsuma, "Rapid detection of inclusion particles in recycled aluminum materials by laser-induced plasma optical emission spectrometry with scanning laser beam," *Surf. Interfaces*, **20** 1-7 (2020). https://doi.org/10.1016/J.SURFIN.2020.100602.
9) Z. Taslicukur, C. Balaban, and N. Kuskonmaz, "Production of ceramic foam filters for molten metal filtration using expanded polystyrene," *J. Eur. Ceram. Soc.*, **27** (*2–3*) 637–640 (2007). https://doi.org/10.1016/J.JEURCERAMSOC.2006.04.129.
10) X. Cao, and J. Campbell, "Oxide inclusion defects in al-si-mg cast alloys," *Can. Metall. Q.*, **44** (*4*) 435–448 (2005). https://doi.org/10.1179/CMQ.2005.44.4.435.
11) Widyantoro, D. Dhaneswara, J. Fajar Fatriansyah, M. Reza Firmansyah, and Y. Prasetyo, "Removal of oxide inclusions in aluminium scrap casting process with sodium based fluxes," *MATEC Web of Conferences*, **269** 07002 (2019). https://doi.org/10.1051/MATECCONF/201926907002.
12) X. Cao, and J. Campbell, "Oxide inclusion defects in al-si-mg cast alloys," *Can. Metall. Q.*, **44** (*4*) 435–448 (2005). https://doi.org/10.1179/CMQ.2005.44.4.435.
13) L.N.W. Damoah, and L. Zhang, "Removal of inclusions from aluminum through filtration," *Metal. Mater. Trans. B*, **41** (*4*) 886–907 (2010). https://doi.org/10.1007/S11663-010-9367-3.
14) Widyantoro, D. Dhaneswara, J.F. Fatriansyah, M. Reza Firmansyah, and Y. Prasetyo, "Removal of oxide inclusions in aluminium scrap casting process with sodium based fluxes," *MATEC Web of Conferences*, **269** 07002 (2019). https://doi.org/10.1051/matecconf/201926907002.
15) S. Kaushik, V. Uniyal, A. Kumar Verma, A. Kumar Jha, S. Joshi, M. Makhloga, P. Singh Pargai, S.K. Sharma, R. Kumar, and S. Pal, "Comparative experimental and cfd analysis of fluid flow attributes in mini channel with hybrid cuo+zno+h2o nano fluid and (H_2O) base fluid," *EVERGREEN*, **10**(1), 182–195 (2023). https://doi.org/10.5109/6781069
16) G. Timelli, and F. Bonollo, "Fluidity of aluminium die castings alloy," *Int. J. Cast Met. Res.*, **20** (*6*) 304–311 (2007). https://doi.org/10.1179/136404608X286110.
17) J. Wannasin, D. Schwam, and J.F. Wallace, "Evaluation of methods for metal cleanliness assessment in die casting," *J. Mater. Process Technol.*, **191** (*1–3*) 242–246 (2007). https://doi.org/10.1016/j.jmatprotec.2007.03.013.
18) C. Stanică, and P. Moldovan, "Aluminum melt

cleanliness performance evaluation using podfa (porous disk filtration apparatus) technology," *UPB Sci. Bull. B: Chem. Mater. Sci.*, **71** (*4*) 107-114 (2009).
19) M. Riestra, A. Bjurenstedt, T. Bogdanoff, E. Ghassemali, and S. Seifeddine, "Complexities in the assessment of melt quality," *Int. J. Met.*, **12** (*3*) 441-448 (2018). https://doi.org/10.1007/s40962-017-0179-y.
20) A.M. Samuel, H.W. Doty, S. Valtierra, and F.H. Samuel, "Inclusion measurements in al–si foundry alloys using qualiflash and prefil filtration techniques," *Int. J. Met.*, **12** (*3*) 625-642 (2018). https://doi.org/10.1007/s40962-017-0185-0.
21) D. Dispinar, and J. Campbell, "Effect of casting conditions on aluminium metal quality," *J. Mater. Process Technol.*, **182** (*1–3*) 405–410 (2007). https://doi.org/10.1016/J.JMATPROTEC.2006.08.021.
22) S. kumar, and A.K. C, "Solid particle erosion performance of multi-layered carbide coatings (wc-sic-cr 3 c 2)," *EVERGREEN*, **10**(2), 813–819 (2023). https://doi.org/10.5109/6792833
23) K. Akhtar, S.A. Khan, S.B. Khan, and A.M. Asiri, "Scanning electron microscopy: principle and applications in nanomaterials characterization," *Handbook of Materials Characterization*, 113–145 (2018). https://doi.org/10.1007/978-3-319-92955-2_4.
24) X. Huang, and H. Yan, "Effect of trace la addition on the microstructure and mechanical property of as-cast ADC12 al-alloy," *J. Wuhan Univ. Technol. Mater. Sci. Ed.*, **28** (*1*) 202-205 (2013). https://doi.org/10.1007/s11595-013-0665-x.
25) W.B.E. Thomsen, and G.J. Roberts, "Spark oes characterizes aluminum mmcs.," *Advanced Materials & Processes*, **155** (*2*) 41–43 (1999). https://go.gale.com/ps/i.do?p=AONE&sw=w&issn=08827958&v=2.1&it=r&id=GALE%7CA54036557&sid=googleScholar&linkaccess=fulltext (accessed October 24, 2023).
26) D.G. Graczyk, D.R. McLain, Y. Tsai, D.B. Chamberlain, and J.L. Steeb, "Correcting nonlinearity and mass-bias in measurements by inductively coupled plasma quadrupole mass spectrometry," *Spectrochim Acta Part B At Spectrosc*, **153** 10–18 (2019). https://doi.org/10.1016/J.SAB.2019.01.003.
27) A. Zulfia, Krisiphala, D. Ferdian, B.W. Utomo, and D. Dhaneswara, "Characteristics of ADC12/nano Al2O3composites with Addition of Ti Produced by Stir Casting Method," in: IOP Conf Ser Mater Sci Eng, (2018). https://doi.org/10.1088/1757-899X/333/1/012046.
28) D. Dhaneswara, K. Wahyudi, M. Anis, J. Aditomo, and J.F. Fatriansyah, "Effect of wood sawdust addition on the morphology, mechanical properties, and thermal properties of mullite-based porous ceramic filter candidates for aluminum casting process," *Appl. Mech. Mater.*, **916** (*4*) 3-9 (2023). https://doi.org/10.4028/p-oGq8iu.
29) M. Anis, K. Wahyudi, J.F. Fatriansyah, N.M. Ariq A., B. Suharno, A. Azhari, and D. Dhaneswara, "Effect of starch content on morphology, mechanical properties, and thermal properties of mullite-based porous ceramic as a candidate filter in aluminum casting," *Appl. Mech. Mater.*, **916** (*1*) 11-18 (2023). https://doi.org/10.4028/p-5YnIKN.
30) Zayad M. Sheggaf, Sharafaddeen S. Wanis Ehzazat, and Almabrouk A. Dhaw Esdeira3, "Fluidity of aluminum piston alloy with different amount of pouring temperature," *J. Humanit. Appl. Sci.*, **8** (*3*) 31-36 (2023). https://doi.org/10.58916/jhas.v8i3.111.
31) Y.E. ASAN, and M. ÇOLAK, "Modeling the effect of pour height, casting temperature and die preheating temperature on the fluidity of different section thicknesses in permanent mold casting of al12si alloys," *Erzincan Üniversitesi Fen Bilimleri Enstitüsü Dergisi*, **15** (*Special Issue I*) (2022). https://doi.org/10.18185/erzifbed.1199648.
32) H. Geng, Q. Xu, S.B. Duraman, and Q. Li, "Effect of rheology of fresh paste on the pore structure and properties of pervious concrete based on the high fluidity alkali-activated slag," *Crystals (Basel)*, **11** (*6*) (2021). https://doi.org/10.3390/cryst11060593.
33) P. Sun, H. Yang, R. Huang, Y. Zhang, S. Zheng, M. Li, and S. Koppala, "The effect of rolling temperature on the microstructure and properties of multi pass rolled 7a04 aluminum alloy," *J. Mater. Res. Technol*, **25** 3200-3211 (2023). https://doi.org/10.1016/j.jmrt.2023.06.123.
34) Z. Zhu, Z. Hu, H.L. Seet, T. Liu, W. Liao, U. Ramamurty, and S.M. Ling Nai, "Recent progress on the additive manufacturing of aluminum alloys and aluminum matrix composites: microstructure, properties, and applications," *Int. J. Mach. Tools Manuf.*, **190** 104047 (2023). https://doi.org/10.1016/j.ijmachtools.2023.104047.
35) J. Cao, C.R. Rambo, and H. Sieber, "Preparation of porous al2o3-ceramics by biotemplating of wood," *J. Porous Mater.*, **11** (*3*) 163–172 (2004). https://doi.org/10.1023/B:JOPO.0000038012.58705.C9/METRICS.
36) K. Akhtar, S.A. Khan, S.B. Khan, and A.M. Asiri, "Scanning electron microscopy: principle and applications in nanomaterials characterization," *Handbook of Materials Characterization*, 113–145 (2018). https://doi.org/10.1007/978-3-319-92955-2_4.
37) D. V Neff, "Improving die casting melt quality and casting results with melt quality analysis and filtration," *Materials Science*, 1-12 (2002).
38) K. Asano, "Mechanical properties of aluminum composites reinforced with pan- and pitch-based short carbon fibers," *Mater. Trans.*, **58** (*6*) 906-913

(2017). https://doi.org/10.2320/matertrans.M2017023.
39) R.J. Dimu, “AC8A aluminum quench modification using banana tree sap fluid,” *International Conference on Applied Science and Technology (ICAST)*, **208** 168–172 (2020). https://doi.org/10.2991/aer.k.211129.038
40) G. Razaz, and T. Carlberg, “Casting practices influencing inclusion distributions in billets,” in: Minerals, Metals and Materials Series, 987-991 (2016). https://doi.org/10.1007/978-3-319-65136-1_167.
41) D. Dhaneswara, J.F. Fatriansyah, N. Hanandhira, A.R. Basa, and M. Reza Firmansyah, “Effect of Sodium Nitrate-Sodium Fluoride Ratio as Degasser in Al-7Si-2Cu Casting Product,” in: IOP Conf Ser Mater Sci Eng, (2019). https://doi.org/10.1088/1757-899X/547/1/012037.